Talanta 85 (2011) 1812–1817

Contents lists available at ScienceDirect

Talanta

journal homepage: www.elsevier.com/locate/talanta

A novel piezoelectric immunosensor for the detection of malarial *Plasmodium falciparum* histidine rich protein-2 antigen

M.K. Sharma, V.K. Rao*, S. Merwyn, G.S. Agarwal, Sanjay Upadhyay, R. Vijayaraghavan

Defence R & D Establishment, Jhansi Road, Gwalior 474002, India

ARTICLE INFO

Article history:
Received 18 April 2011
Received in revised form 4 July 2011
Accepted 6 July 2011
Available online 14 July 2011

Keywords:
*Pf*HRP-2 antigen
Malaria
Piezoelectric quartz crystal
SAMs
Immunosensor

ABSTRACT

A novel piezoelectric (PZ) immunosensor for the direct detection of malarial *Plasmodium falciparum* histidine rich protein-2 (*Pf*HRP-2) antigen was developed. The mixed self-assembled monolayers (SAMs) of thioctic acid and 1-dodecanethiol were formed on gold surface of quartz crystal. Cyclic voltammetry, electrochemical impedance spectroscopy and surface Raman spectroscopy techniques were used to characterize the mixed SAMs. The rabbit anti-*Pf*HRP-2 antibodies were coupled on mixed SAM modified gold surface of quartz crystal via NHS/EDC activation method. The PZ immunosensor was applied to detect *Pf*HRP-2 in the linear range of 15–60 ng/ml with a detection limit of 12 ng/ml. It was also found that even after 14 days of storage, 50% of the activity still remained. Clinical human serum samples were tested with this method, and the results were in agreement with those obtained from commercially available ICT kit (NOW® Malaria).

1. Introduction

The development of a rapid, simple, label-free method for the detection of proteins has been a long-standing goal for researchers. Piezoelectric (PZ) immunosensing methods, being a label-free assay can offer an alternative to existing methods. Methods based on the use of PZ crystals have been developed for the detection of bacteria [1,2], virus [3] and toxins [4,5]. The piezoelectric (PZ) immunosensor is an application of Sauerbray's equation, which describes the relationship between the resonant frequency of a crystal and mass deposited on its electrodes:

$$\Delta F = \frac{-2.3 \times 10^6 F^2 \Delta M}{A}$$

where ΔF is the measure frequency shift (Hz), F is the resonant frequency of the PZ crystal (MHz), A is the area of the coated crystal and ΔM is mass change (g/cm^2) due to surface deposition. The system functions as quartz crystal microbalance (QCM). The amount of molecules bound on the sensitive area of the electrodes can be quantitatively measured as a decrease in resonant frequency.

Antibody immobilization is a crucial step in the successful development of a PZ immunosensor. The immobilization process must preserve the biological activity of the antibody and an efficient binding. The self-assembled monolayer (SAM) technique is the simplest way to provide a well ordered layer for the modification of electrode surface with antibodies to improve the detection sensitivity, speed and reproducibility [6,7]. Sulfur containing molecules such as dialkane disulfides (R–SS–R), sulfides (R–S–R) and alkyl thiols form highly ordered SAMs on the metal surfaces. Among all these, alkylthiols spontaneously chemisorb on gold surfaces and form densely packed thiolate films in a very reproducible manner [8,9]. Mercaptoacetic acid (MAA) and mercaptopropionic acid (MPA) have been reported to create carboxylic acid functionalized monolayers after activation with EDC and NHS for the attachment of proteins [10–13]. 11-Mercaptoundecanoic acid (MUA) has also been explored to prepare SAMs on a quartz surface due to its high dielectric property [14,15]. The ω-functionalized thiols, such as thioctic acid (TA), with bulky group (COOH, ferrocene) decrease the density of packing and ordering of monolayer [16–18]. The TA is molecule containing disulfide base, which helps for its strong adsorption on the gold surface. On the other hand, TA alone forms poor SAMs due to hydrogen bonding between neighboring molecules with the tilt angle of 38° that corresponds to the loose packing of SAMs.

Therefore, mixed SAMs have been explored to improve the sensitivity via proper orientation of antibodies immobilized on such layers [19,20]. Mixed SAMs generally consists of one thiolate with a functional head group like carboxylic acid and another long chain alkyl thiolate as a diluent [21–24]. Mixed SAMs consisting of alkyl thiols with over 10 carbons in the alkyl chain form a densely packed crystalline-like monolayer assembly with extended all-trans alkyl chain tilted 20–30° the surface normal [25]. No phase segregation occurs when active thiol is adsorbed together with the long chain thiol due to strong hydrophobic interactions between the alkyl

* Corresponding author.
E-mail address: vepakrao@yahoo.com (V.K. Rao).

0039-9140/$ – see front matter © 2011 Elsevier B.V. All rights reserved.
doi:10.1016/j.talanta.2011.07.008

chains [26]. Mixed SAMs show more heterogeneous layers with phase segregation, when the chain lengths of adsorbed thiols differ by more than four carbons [27,28].

The *P. falciparum* parasite is a major cause of malaria in humans. It synthesizes several proteins known as *P. falciparum* histidine rich proteins (*Pf*HRPs). One of these, *Pf*HRP-2 is found in high density in infected blood of patients. In recent years, various methods for the detection of malaria have been reported, such as immunochromatographic tests (ICT) [29,30], immunofluorescent antibody test (IFAT) [31], enzyme linked immunosorbent assay (ELISA) [32], polymerase chain reaction (PCR) [33], laser light-scattering immunoassay [34] and chemodetection [35]. All these reported methods are time consuming, labour intensive and require significant materials.

Recently, our group has reported amperometric immunosensors as alternative to conventional methods for malarial *Pf*HRP-2 detection using alkaline phosphatase (AP) enzyme as label [36,37]. Although, these amperometric immunosensors are highly sensitive but require labels, several incubation and washing steps. Till date, no report is available for the label-free detection of malarial *Pf*HRP-2 based on PZ immunosensing. In the present study, for the first time we are reporting on the development of PZ immunosensor for the detection of malarial *Pf*HRP-2 antigen based on mixed SAMs of thioctic acid (TA) and 1-dodecanethiol (DDT). The rabbit anti-*Pf*HRP-2 antibodies (capturing antibody) were coupled on mixed SAM modified crystal via NHS/EDC activation method. The developed immunosensor is sensitive and retains stability for longer time.

2. Material and methods

2.1. Reagents

Coupling agents, 1-ethyl-3-(3-dimethylaminopropyl) carbodiimide hydro-chloride (EDC), N-hydroxysuccinimide (NHS), DL-thioctic acid (TA) and 1-dodecanethiol (DDT) were obtained from Acros organics, USA. Piranha solution was prepared by mixing 3:1 concentrated sulfuric acid to 30% hydrogen peroxide solution. 0.5 M KOH was prepared by dissolving 2.8 g KOH in 100 ml double distilled water. Activation solution was prepared by dissolving 10 mM EDC and 20 mM NHS in 25 ml double distilled water. 3 mM TA and 9 mM DDT were prepared in absolute ethanol. All other chemicals used were of analytical grade. Human clinical samples were collected from patients with fever (malaria-like symptoms) local hospital in Gwalior (India). After it, samples were processed for serum separation and stored at 4 °C. NOW Malaria® test was conducted at the sample collection site. Thick and thin smears of the suspected patients were prepared for microscopic examination. For amperometric immunosensing serum samples were brought to laboratory.

2.2. Apparatus

The electrochemical measurements were carried out on a PGSTAT-302 Potentiostat obtained from Autolab with GPES software (Eco Chemie). A conventional three-electrode system comprising electrode (diameter = 2 mm) as working electrode after modification with mixed SAMs (TA + DDT), platinum wire as auxiliary electrode and Ag/AgCl electrode as a reference electrode were used. All experiments were performed at room temperature (25 ± 1 °C). Raman system (Renishaw, United Kingdom) was utilized in this study. Frequency monitor (model PM 701) and 5 MHz AT-cut, gold coated quartz crystals were procured from Maxtek, USA. Commercially available NOW® Malaria, ICT kit (Binax, Inc. US) was also utilized.

2.3. Preparation of HRP-2 of P. falciparum by recombinant DNA technology

The procedure for the preparation of the antigen is described here briefly. DNA was extracted from cultured *P. falciparum* by processing the infected RBC's with QIAamp DNA blood mini kit as per the manufacturer's instructions. *Pf*HRP-2 gene sequence was amplified by polymerase chain reaction (PCR) and purified. The purified PCR product was cloned in pQE-30 UA cloning vector. *Escherichia coli* strains M15 was used for the transformation and expression of Histidine fusion protein. Purification of expressed *Pf*HRP-2 protein was carried out by Ni-NTA affinity chromatography in native conditions using commercially available Ni-NTA columns (Qiagen, Germany) as per the manufacturer's instructions. Briefly, the harvested cells were lysed in a sonicator and the soluble recombinant protein with the histidine tag was captured onto the Ni^{2+} ions in Ni-NTA resin (The amino acid histidine in the histidine tag of the recombinant protein have affinity towards Ni^{2+} ions in Ni-NTA resin). After, a brief washing the protein was eluted using 350 mM imidazole. The purity of the *Pf*HRP-2 was examined for any contaminating proteins by sodium dodecyl disulphate-poly acrylamide gel electrophoresis (SDS-PAGE) analysis. The protein content was determined by Lowery method and found to be 758 μg/ml.

2.4. Preparation of polyclonal antiserum

The New Zealand white rabbits were used for raising hyper immune sera against recombinant *Pf*HRP-2 antigen. The rabbits were initially immunized by subcutaneous route with 100 μg of recombinant antigen and freund's complete adjuvant (FCA) at four different sites. They were subsequently boosted with 100 μg of antigen along with freund's incomplete adjuvant (FIA) intramuscularly at 15 days interval for 45 days. The rabbits were bled from the heart, sera was separated and stored at −20 °C.

2.5. Immunoglobulins (IgGs) purification

Five ml of saturated ammonium sulphate was added drop wise and slowly to 5 ml of 1:1 diluted hyper immune serum and stirred for 30 min. The precipitated proteins (IgGs) were removed by centrifugation at 5000 rpm for 10 min at 4 °C. The precipitated IgGs were washed with 1:1 v/v saturated ammonium sulphate twice to remove remaining soluble proteins. The precipitate was dissolved in 1 ml of 0.1 M PBS, pH 7.2 and desalted by dialysis.

2.6. Formation of the mixed self-assembled monolayer

Prior to formation of mixed SAM, gold coated quartz crystals (5 MHz) were cleaned by dipping in to a hot piranha solution for 45 s and washed with distilled water. In the next step, it was immersed in a binary mixture of 3 mM of TA and 9 mM DDT in absolute ethanol for 4 h and thoroughly rinsed in ethanol and air-dried.

2.7. Immobilization of antibodies on gold coated quartz crystal

The mixed SAM modified electrodes were activated by immersing in a solution containing 10 mM EDC and 20 mM NHS in double distilled water for 2 h at room temperature. After it, the electrodes were washed with double distilled water and then dipped in a solution containing of 300 μg/ml rabbit anti-*Pf*HRP-2 antibody for 1 h to achieve the complete binding. The crystal was then rinsed with tris buffer (pH 7.2) and air-dried. Further, 50 μl of 3% BSA was added on to the antibody modified electrode surface to prevent non-specific binding and incubated for 30 min at 37 °C. After rinsing with tris

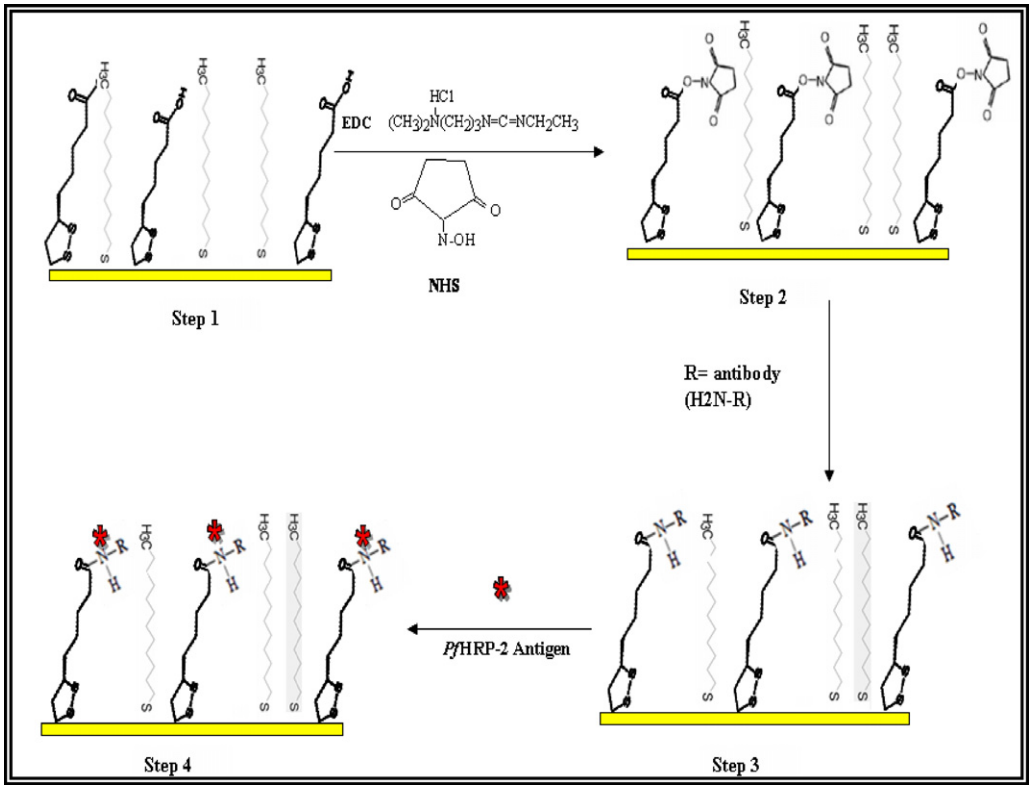

Fig. 1. Schematic diagram for piezoelectric immunosensor preparation.

buffer, pH 7.2 and distilled water, the modified crystals were stored at 4 °C in tris buffer pH 7.2.

2.8. Measurement with QCM

The antibody immobilized crystal was air-dried and then fixed onto the crystal holder. Then, it was immersed in a glass cell containing 50 ml of tris buffer, pH 7.2. It was kept in glass cell for a time period and measured the stable frequency of ±1 Hz. Different concentrations of *Pf*HRP-2 antigen were then added to this solution and the change in frequency was monitored.

3. Results and discussions

3.1. Formation of SAM and the biosensing layer

The successive steps of SAM and biosensing layer formation are depicted in Fig. 1. Step 1 is the co-adsorption of two thiols, DDT and TA to form mixed SAM; step 2 is the activation of the crystal surface by NHS and EDC to provide high sensitivity and good reproducibility; step 3 is the covalent immobilization of rabbit anti-*Pf*HRP-2 antibodies followed by blocking with 3% BSA to prevent the non-specific binding; step 4 is the formation of immuno-complex by adding 10 μl of *Pf*HRP-2 antigen onto the coated and blocked crystal.

3.2. Electrochemical characterization of the self-assembled monolayers

Cyclicvoltammetry (CV) and electrochemical impedance spectroscopy (EIS) techniques were employed to study the interface properties of the modified crystal surface. CV and EIS experiments were performed on pure gold electrode (diameter 2 mm). Fig. 2 shows the relative CV responses for modified and unmodified gold electrodes, i.e. Bare Au, TA/Au, DDT/Au and Mixed SAM (TA + DDT)/Au in 5 mM $Fe(CN)_6^{3-/4-}$ containing 0.1 M KCl solution. In the case of bare Au a well-defined oxidation and reduction peaks with peak-to-peak separation of ΔEp of 97 mV was observed (Fig. 2, curve a). After depositing SAM on Au electrode with TA, i.e. TA/Au, significant decrement in redox peak was observed (Fig. 2, curve b). It appeared that the TA SAM layer blocked the electrode surface for diffusion of ferricyanide. However, DDT/Au electrode showed drastic decrement in redox peak than that of TA SAM (Fig. 2, curve c). SAMs with long alkanethiols ($n > 10$) cause a dramatic decrease in electrode/electrolyte capacitance compared with bare gold [38]. In the case of mixed SAM (TA + DDT)/Au, the electrode surface is almost covered (Fig. 2, curve d). This high insulating behaviour of the thin layer of mixed SAM was due to the combined effect of TA and DDT. This insulating layer prevented the oxidation–reduction reaction on the gold electrode surface.

EIS was also employed to characterize the interface properties of the modified Au electrodes. In a typical Nyquist plot, the semicircle portion corresponds to the electron-transfer resistance (Ret) at higher frequency range while at lower frequency range represents the diffusion limited process. In the present work, EIS study of the modified electrodes was carried out in 1.0 mM $Fe(CN)_6^{3-/4-}$ containing 0.1 M KCl solution with a frequency range of 10 mHz–1 MHz. As shown in Fig. 3A, the Ret value ~600 Ω corresponds to the bare Au electrode (Fig. 3A, curve b). After deposition of TA SAM, the EIS of the resulting layer shows semicircle domain with Ret ~17 kΩ (Fig. 3A, curve a) suggesting that TA SAM layer blocked the redox probe to diffuse towards the gold electrode surface. On the other hand, higher Ret values (~1.5 MΩ) were observed in the case of DDT/Au electrode (Fig. 3B, curve b). As expected, charge transfer and diffusion of the redox probe through the DDT SAM is more inhibited than through the TA SAM. This involves a reduction in noise and a relative enhancement of the faradaic current (provided that this current is not significantly attenuated

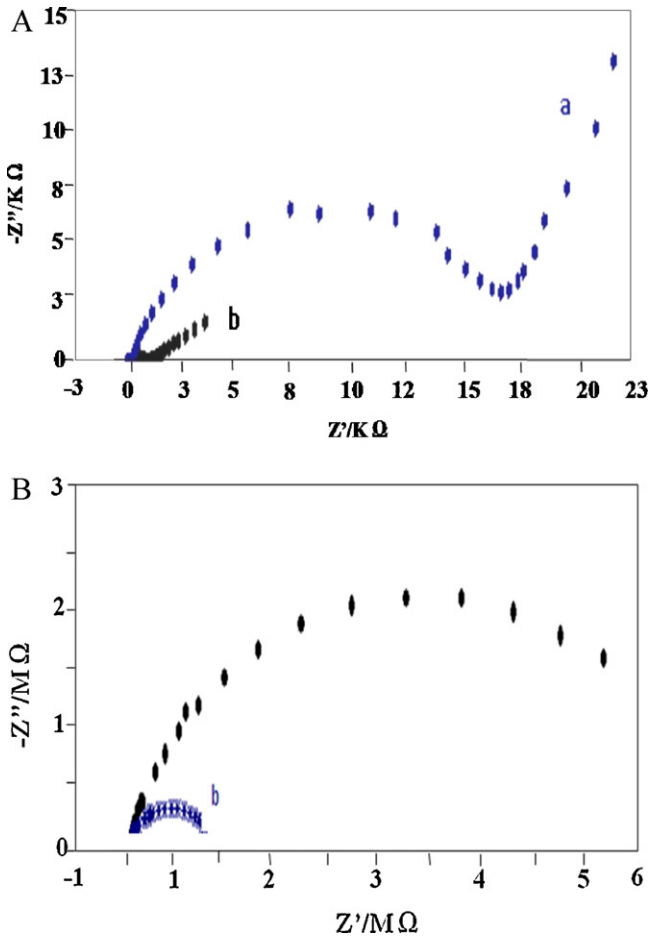

Fig. 2. Cyclic voltammograms measured with bare Au (a); TA/Au (b); DDT/Au (c); and mixed SAM (TA + DDT)/Au (d) in a solution containing 5 mM $Fe(CN)_6^{3-/4-}$ with 0.1 M KCl; scan rate 10 mV s^{-1}.

by the monolayer). It can be seen that (Fig. 3B, curve a) mixed SAM (TA + DDT)/Au has shown very high Ret value (~5.5 MΩ). These results were in agreement with to CV data as shown in Fig. 2.

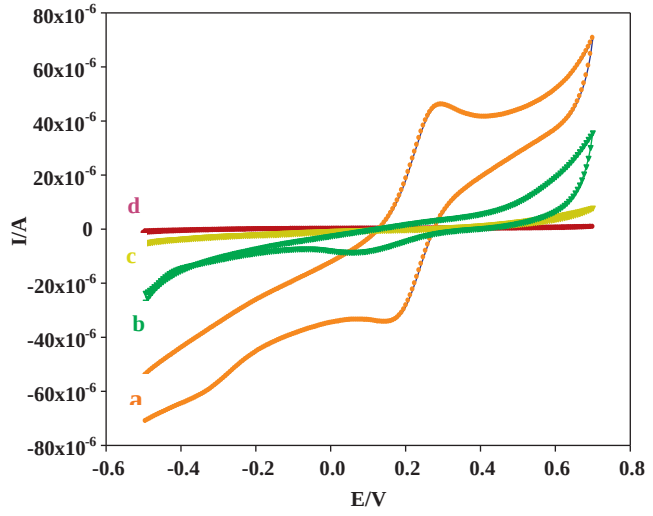

Fig. 3. Nyquist plots: [A] TA/Au (a) and clean Au electrode (b); [B] mixed SAM (TA + DDT)/Au electrode (a) and DDT/Au electrode. Measured in 1.0 mM Fe (II/III) redox couple, f = 1 MHz–10 mHz, E_{dc} = +0.2 V, E_o = 10 mV.

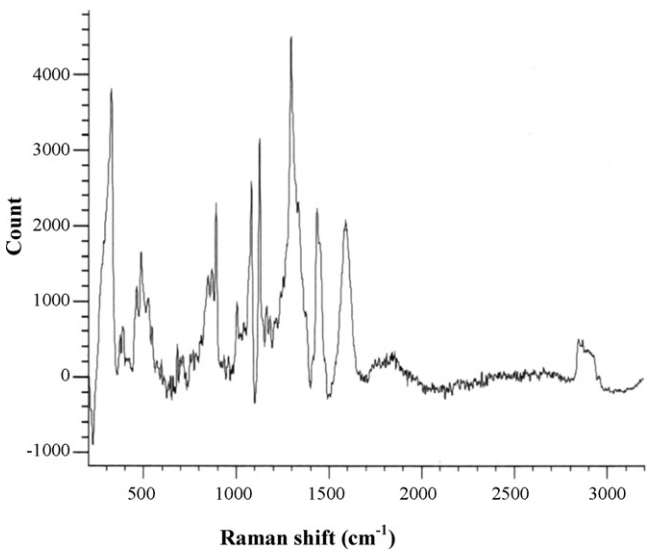

Fig. 4. Surface Raman spectrum of mixed SAM (TA + DDT)/Au electrode; laser source 784 nm; exposure time 10 s.

3.3. Raman spectrum of mixed SAMs

Fig. 4 displays the Raman spectrum of the gold surface after immersion in a mixture of TA and DDT. The formation of a covalent gold–sulfur bond has been proven by the presence of the large band in the range of 500–700 cm^{-1}. This large band is assigned to stretch the mode of C–S groups. Vibration bands in the lower wave number range were also observed at 1400 and 1650 cm^{-1} showing the presence of acidic groups, mainly in the deprotonated form. The peak observed at 1320 cm^{-1} is assigned to the C–H vibration mode. Finally, a small main band at 2900–2950 cm^{-1} is clearly observed in the high frequency region. This is assigned to the vibration mode of alkyl thiol chains. These findings provide good evidence that adsorption of the mixed SAM of TA and DDT did occur.

3.4. Rabbit anti-PfHRP-2 (capturing antibody) amount optimization

The amount of antibody to be immobilized plays an important role on frequency change. More the amount of capturing antibody bound to the crystal greater would be the response/frequency shift but on the other hand over loading leads to the lowering of the response. In the present study, the immobilization time was fixed at 1 h. The frequency shift (ΔF) values increases with increase in concentration of capturing antibody. In this case, the ΔF value increases with the increase of antibody concentration from 0.1 to 300 μg/ml and begin to decrease thereafter (Table 1). This demonstrated that 300 μg/ml of antibody concentration is required for the complete coverage of electrode surface in 1 h. Therefore, optimized

Table 1
Change in frequency with the rabbit anti-*Pf*HRP-2 antibody (capturing antibody) concentration.

Concentration of antibody (μg/ml)	Antibody immobilization ΔF (Hz)
10	62 ± 3
50	89 ± 3
100	101 ± 5
200	123 ± 6
250	139 ± 8
300	146 ± 9
350	141 ± 8
400	138 ± 6

Table 2
The comparison of results given by PZ immunosensor and ICT (NOW® Malaria) method.

Human clinical serum samples	Sample no. 1	Sample no. 2	Sample no. 3	Sample no. 4	Sample no. 5	Sample no. 6	Negative sample
PZ immunosensor (ng/ml)[a]	25	55	40	55	30	15	Nil
Frequency change (Hz)	98	156	149	156	116	58	19
NOW® Malaria	weak +ve	+ve	+ve	+ve	+ve	weak +ve	−ve

[a] The average value of three successive determinations, these values are very higher (more than detection limit of immunosensor, i.e. 12 ng/ml). These are real samples and the concentrations (ng/ml) for each sample was quantified based on the calibration plot as described in Fig. 5.
+ve: the sample is positive for malarial infection.
−ve: the sample is negative for malarial infection.

amount of capturing antibody, i.e. 300 μg/ml was utilized in further studies.

3.5. Calibration curve for PfHRP-2

The calibration curve for *Pf*HRP-2 was obtained by applying *Pf*HRP-2 solution of various concentrations to the antibody-coated crystals for 1 h at 37 °C (Fig. 5). The experimental results were approximated by sigmoid function and non-linear fitting was used for mathematical equation expression. The generalized mathematical equation for this sigmoid curve was $y = -15.09 + 176.6/(1 + \exp(-(x - 19.5)/88.37))$ with a correlation coefficient of $r^2 = 0.996$. From this sigmoid curve, the linear range of the PZ immunosensor was found to be 15–60 ng/ml. The detection limit was found to be 12 ng/ml with a frequency response of 37 Hz ($n = 3$), which is larger than three-time standard deviation of control experiment (±7.0 Hz).

3.6. Evaluation of immunosensor against human clinical samples

The feasibility of applying the developed sensor in clinical systems was investigated via analyzing human clinical samples, and comparing with the commercially available ICT kit (NOW® Malaria, Binax, Inc. US). These samples were diluted (1:100) prior to apply into developed immunosensor and ICT kit to minimize the effect of serum on the response. The comparison between the results of the proposed immunosensor and the NOW® Malaria ICT kit was shown in Table 2. From the results, it is suggested that that there was no difference between the results given by the two methods. Therefore, the proposed immunosensor could be reasonably applied in the clinical determination of *Pf*HRP-2 antigen. It may be noted that at concentration less than 25 ng/ml, the NOW® Malaria ICT kit gives a weak signal (or color indication) while immunosensor provides sound response.

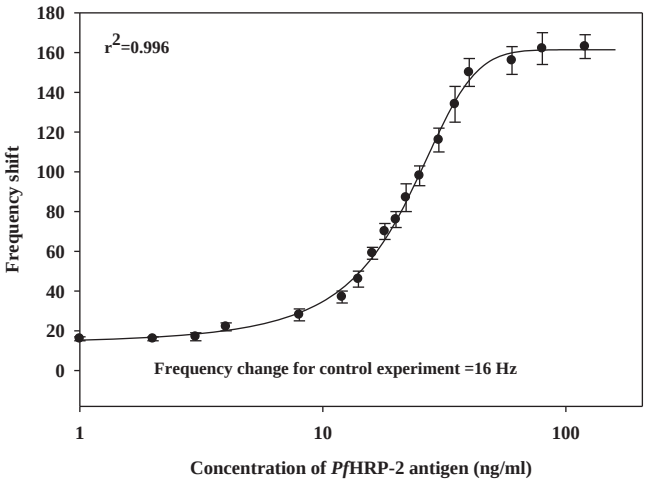

Fig. 5. Calibration plot (log concentration of *Pf*HRP-2 vs. change in frequency) for the PZ immunosensor for malarial *Pf*HRP-2 antigen.

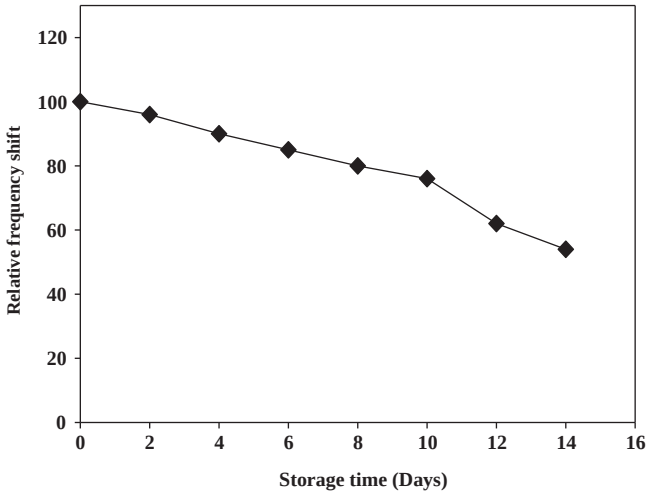

Fig. 6. Stability study of *Pf*HRP-2 piezoimmunosensor, responses were measured for 40 ng/ml of *Pf*HRP-2 antigen.

3.7. Reproducibility and stability of PfHRP-2 piezoimmunosensor

Reproducibility performances of the rabbit anti-*Pf*HRP-2 modified crystal were studied. For this purpose, 5 mM glycine–HCl buffer solution (pH 2.8) was used to break the affinity binding between *Pf*HRP-2 antigen and anti-*Pf*HRP-2 antibody. The *Pf*HRP-2 antigen (40 ng/ml, $\Delta F = 162$ Hz at first experiment) was detected by the regenerated crystal surface by monitoring the change of frequency signal. After, 32 times of regeneration the binding activity of anti-*Pf*HRP-2 retained more than 91% ($\Delta F = 149$ Hz) of original frequency change (frequency shift 162 Hz) with the relative standard deviation (R.S.D.) of 3.6%.

The developed PZ immunosensor was also evaluated in terms of stability. For this purpose crystal were coated with optimized amount of rabbit anti-*Pf*HRP-2 antibody. The quartz crystals were kept in a dry condition at 4 °C and tested at regular intervals up to 14 days. The frequency change observed upon the addition of *Pf*HRP-2 solution (40 ng/ml) and was used as a measure of the stability of the crystals. The relative frequency shift data are shown in Fig. 6. There was no significant change in the resonant frequencies in the first 2 days but after it, a gradual decline was resulted. The activity was still retained at the level of 50% even after 14 days storage of antibody-coated crystal kept at 4 °C.

4. Conclusions

In this work, a PZ immunosensor was developed for the direct detection of malarial *Pf*HRP-2 antigen. Covalent coupling of anti-*Pf*HRP-2 antibodies on mixed SAM (TA + DDT) modified gold surface was carried out with NHS/EDC. The properties of TA (strong adsorption on gold surface due to disulfides) and DDT (dense packing of monolayers due to long carbon chain length) were explored as mixed SAMs for malarial *Pf*HRP-2 detection. The detection limit was

found to be 12 ng/ml. It was also found that even after 14 days of storage 50% of the activity still remained. The binding activity of anti-*Pf*HRP-2 retained more than 91% of original frequency change after the 32 times of regeneration. Finally, this study demonstrated that it is feasible to detect of malarial *Pf*HRP-2 antigen with the proposed PZ immunosensor. However, it is slightly less sensitive than our earlier report on amperometric immunosensing of malarial antigen [37]. Since, it is label less and reusable, the sensitivity could be compensated to some extent.

Acknowledgements

The authors are thankful to Dr. N. Gopalan, Dr. G. P. Rai and Dr. Shri Prakash for their support.

References

[1] X.L. Su, Y. Li, Biosens. Bioelectron. 19 (2004) 563–574.
[2] Y.Y. Wong, S.P. Ng, M.H. Ng, S.H. Si, S.Z. Yao, Y.S. Fung, Biosens. Bioelectron. 17 (2002) 676–684.
[3] A.J.C. Eun, L.Q. Huang, F.T. Chew, S.F.Y. Li, S.M. Wong, Phytopathology 92 (2002) 654–658.
[4] J. Homola, J. Dostalek, S.F. Chen, A. Rasooly, S.Y. Jiang, S.S. Yee, Int. J. Food Microbiol. 75 (2002) 61–69.
[5] H.C. Lin, W.C. Tsai, Biosens. Bioelectron. 18 (2003) 1479–1483.
[6] T. Hianik, M. Snejdarkova, L. Sokolikova, E. Meszar, R. Krivanek, V. Tvarozek, I. Novotny, J. Wang, Sens. Actuators B 57 (1999) 201–212.
[7] Y.S. Fung, Y.Y. Wong, Anal. Chem. 73 (21) (2001) 5302–5309.
[8] C.D. Bain, E.B. Troughton, Y.T. Tao, J. Evall, G.M. Whitesides, R.G. Nuzzo, J. Am. Chem. Soc. 111 (1989) 321–335.
[9] K.D. Truong, P.A. Rowntree, J. Phys. Chem. 100 (1996) 19917–19926.
[10] S. Zhang, J. Ding, Y. Liu, J. Kong, O. Hofstetter, Anal. Chem. 78 (2006) 7592–7596.
[11] T. Deng, H. Wang, L.J. Shan, S.G. Li, Y.R. Qin, Anal. Chim. Acta 532 (2005) 137–144.
[12] Z.Y. Wu, G.L. Shen, S.P. Wang, R.Q. Yu, Anal. Sci. 19 (2003) 437–440.
[13] N. Adanyi, M. Varadi, N. Kim, I. Szendro, Curr. Appl. Phys. 6 (2006) 279–286.
[14] A. Tlili, A. Abdelghani, S. Hleli, M.A. Maaref, Sensors 4 (2004) 105–114.
[15] E. Briand, M. Salmain, J.M. Herry, H. Perrot, C. Compere, C.M. Pradier, Biosens. Bioelectron. 22 (2006) 440–448.
[16] J. Lahiri, L. Isaacs, G.M. Whitesides, Anal. Chem. 71 (1999) 777–790.
[17] M. Wirde, U. Gelius, L. Nyholm, Langmuir 15 (1999) 6370–6378.
[18] A.J. Guiomar, J.T. Guthrie, S.D. Evans, Langmuir 15 (1999) 1198–1207.
[19] F. Frederix, K. Bonroy, W. Laureyn, G. Reekmans, A. Campitelli, W. Dehean, G. Maes, Langmuir 19 (2003) 4351–4357.
[20] B. Ge, F. Lisdat, Anal. Chim. Acta 454 (2002) 53–64.
[21] D. Hobara, T. Sasaki, S. Imabayashi, T. Kakiuchi, Langmuir 15 (1999) 5073–5078.
[22] L. Li, S. Chen, S. Jiang, Langmuir 19 (2003) 666–671.
[23] E. Cooper, G.J. Leggett, Langmuir 15 (1999) 1024–1032.
[24] H.Y. Liu, S.G. Liu, L. Echegoyen, Chem. Commun. 16 (1999) 1493–1494.
[25] A. Ulman, J.E. Eilers, N. Tillman, Langmuir 5 (1987) 1147–1152.
[26] R.S. Clegg, J.E. Hutchison, J. Am. Chem. Soc. 121 (1999) 5319–5327.
[27] S. Chen, L. Li, C.L. Boozer, S.J. Jiang, Phys. Chem. B 105 (2001) 2975–2980.
[28] T. Kakiuchi, M. Iida, N. Gon, D. Hobara, S.I. Imabayashi, K. Niki, Langmuir 17 (2001) 1599–1603.
[29] R.F.G. Leke, R.R. Djokam, R. Mbu, R.J. Leke, J. Fogako, R. Megnekou, S. Metenou, G. Sama, Y. Xhou, T. Cadigan, M. Parra, D.W. Taylor, J. Clin. Microbiol. 37 (1999) 2992–2996.
[30] C.J. Shiff, Z. Premji, J.N. Minjas, Trans. R. Soc. Trop. Med. Hyg. 87 (1993) 646–648.
[31] M.E. De Carvalho, M.U. Ferreira, M.R. De Souza, R.T. Ninomia, G.F. Matos, L.M. Camargo, C.S. Ferreira, Mem. Inst. Oswaldo Cruz 87 (2) (1992) 205–208.
[32] V. Namsiripongpun, H. Wilde, P. Pamsandang, P. Tiersansern, Trans. R. Soc. Trop. Med. Hyg. 87 (1993) 32–34.
[33] D.M. Whiley, G.M. LeCornec, A. Baddeley, J. Savill, M.W. Syrmis, I.M. Mackay, D.J. Siebertb, D. Burnsb, M. Nissend, T.P. Sloots, Diagn. Microbiol. Infect. Dis. 49 (2004) 25–29.
[34] P.A. Demirev, A.B. Feldman, D. Kongkasuriyachi, P. Scholl, D. Sullivan, N. Kumar, Anal. Chem. 74 (2002) 3262–3266.
[35] D. Sahal, R. Kannan, A. Sinha, P. Babbarwal, B.G. Prakash, G. Singh, V.S. Chauhan, Anal. Biochem. 308 (2004) 405–408.
[36] M.K. Sharma, G.S. Agarwal, V.K. Rao, S. Upadhyay, S. Merwyn, N. Gopalan, G.P. Rai, R. Vijayaraghavan, S. Prakash, Analyst 135 (2010) 608–614.
[37] M.K. Sharma, V.K. Rao, G.S. Agarwal, G.P. Rai, N. Gopalan Shri Prakash, S.K. Sharma, R. Vijayaraghavan, J. Clin. Microbiol. 46 (11) (2008) 3759–3765.
[38] H.O. Finklea, S. Avery, M. Lynch, T. Furtsch, Langmuir 3 (1987) 409–413.